








Article

Synthesis and Characterization of Electrospun Sorbent for the Solid-Phase Extraction of Fluoroquinolones in Human Plasma and Their UHPLC-PDA Determination

Vincenzo Ferrone ¹, Giuseppe Carlucci ^{1,*}, Pantaleone Bruni ¹, Lisa Marinelli ¹, Pasquale Avino ², Edoardo Milanetti ³, Serena Pilato ¹, Leonardo Sbrascini ⁴, Pietro Di Profio ¹ and Stefania Ferrari ¹

¹ Department of Pharmacy, University “G. d’Annunzio” of Chieti-Pescara, I-66100 Chieti, Italy

² Department of Agricultural Environmental and Food Science (DiAAA), University of Molise, Via De Sanctis, I-86100 Campobasso, Italy

³ Department of Physics, University “La Sapienza”, Ple A. Moro, 5, I-00185 Roma, Italy

⁴ Chemistry Division, School of Science and Technologies, University of Camerino, I-62032 Camerino, Italy

* Correspondence: giuseppe.carlucci@unich.it

Abstract: In this work we investigated the synthesis and the characterization of electrospun polyacrylonitrile (PAN) and polymethyl methacrylate (PMMA) stabilized in air, made in a 5:1 ratio, used as sorbent for the solid-phase extraction of fluoroquinolones in plasma samples and the following quantification in UHPLC-PDA. Preliminary analyses of viscosity were carried out on the polymer solution to be sure about the electrospinability. Characterizations were performed on the electrospun membrane to evaluate the morphology (SEM scanning electron microscopy and AFM atomic force microscopy), the thermal degradation behavior (TGA thermogravimetric analysis), the porosity and the surface area (BET, Brunauer Emmett Teller), and the quantitative and qualitative distribution of atomic structures (FTIR infrared analysis in Fourier transform and EDX Energy Dispersive X-ray analysis). A solid-phase extraction method was developed by studying parameters such as the amount of sorbent and the pH of the sample. Finally, a UHPLC-PDA method for the analysis of fluoroquinolones was developed and validated in accordance with the guidelines and successfully applied. The use of the prepared sorbent combined with UHPLC-PDA has allowed the development of a method whose strengths are its speed, accuracy, sensitivity, and high recoveries.

Keywords: electrospun sorbent; solid-phase extraction; fluoroquinolones; UHPLC-PDA; method development; electrospinning



Citation: Ferrone, V.; Carlucci, G.; Bruni, P.; Marinelli, L.; Avino, P.; Milanetti, E.; Pilato, S.; Sbrascini, L.; Di Profio, P.; Ferrari, S. Synthesis and Characterization of Electrospun Sorbent for the Solid-Phase Extraction of Fluoroquinolones in Human Plasma and Their UHPLC-PDA Determination. *Separations* **2023**, *10*, 104. <https://doi.org/10.3390/separations10020104>

Academic Editor: Ki Hyun Kim

Received: 30 December 2022

Revised: 20 January 2023

Accepted: 28 January 2023

Published: 2 February 2023



Copyright: © 2023 by the authors. Licensee MDPI, Basel, Switzerland. This article is an open access article distributed under the terms and conditions of the Creative Commons Attribution (CC BY) license (<https://creativecommons.org/licenses/by/4.0/>).

1. Introduction

Fluoroquinolones (FLQs) were obtained starting from quinolones by adding a fluorine atom in position 6 and a piperazine in position 7, giving the compound a different spectrum of activity [1]. These compounds target two enzymes, bacterial gyrase and DNA topoisomerase IV, and by binding to them, they inhibit the resealing of bacterial DNA, interfering with the processes of DNA repair and replication and transcription, leading to the death of the bacterial cell. Several studies showed that the broad-spectrum bactericidal action of fluoroquinolones is concentration-dependent [2].

Furthermore, the most important predictor of clinical cure has been shown to be the relationship between the ratio of the 24 h area under the concentration–time curve and MIC [3]. Consequently, adequate monitoring of fluoroquinolone plasma concentrations is important to prevent bacterial resistance. Finally, to facilitate routine clinical practice, it is essential to use sample preparation techniques that are quick, simple, and adequate [4].

Sample preparation in a chemical analysis is the most time-consuming procedure. The final aim of sample preparation is to improve sensitivity and reproducibility and finally to bring analytes from a solid or liquid matrix into a suitable solvent with the instrumentation [5,6].

In the last two decades, sorbent-based extraction techniques and their miniaturization have gradually found more and more application, replacing liquid–liquid extraction in the analyses of xenobiotics from biological, environmental, and food matrices [7,8].

Solid-phase extraction (SPE) is a widely used sample preparation technique with principles similar to those of high-performance liquid chromatography [9].

A typical disposable SPE cartridge is usually made of medical-grade polypropylene equipped with a Luer tip to direct the effluent into a small container or vial if a needle is affixed. The frits that hold the particle bed in the cartridge are made of polyethylene, PTFE, or stainless steel with a porosity of 10–20 μm , and therefore they offer little flow resistance [10].

An ideal sorbent has several characteristics, such as low cost, easy preparation, and high selectivity. Furthermore, it must guarantee a high adsorption capacity due to the competition between analytes and interferents in the interaction with the sorbent. The parameters affecting the extraction procedure are influenced by the chemical structure and type of absorbent, the adsorption, the separation procedure, and the elution solvent [11].

In the last ten years, micro-extraction techniques or, alternatively, the application of new materials to already existing sample preparation techniques have increasingly attracted the attention of the scientific community [12].

Particularly, in the field of adsorbents, electrospun fibers have had a great impact due to their unique physicochemical and mechanical properties and their huge chemically active surfaces [13,14]. The electrospinning technique allows the production of ultrathin fibers with controlled diameter, size, morphology, and composition, charging the polymer solutions and directing them towards a collection manifold in a very homogeneous way. Briefly, in this technique, an electrical jet of spinning solution is produced by applying a high voltage between a needle and a collector. The micro-nanofiber is obtained when the repulsion of the surface charge of the solution exceeds its surface tension [15].

Based on their morphology, nanofibers can be classified as core-shell, hollow, and porous materials. Electrospun nanofibers have extraordinary characteristics such as a high functionalizable surface area, a high mechanical performance, a high porosity, and a good permeability to gases and liquids, all excellent elements that make them perfect candidates to be an SPE absorbent [16].

Through electrospinning it was possible to use different types of materials, in particular polymers, thanks to the ease and handling of the processing, taken individually or in combination [17].

PAN was one of the most synthetic polymers used in electrospinning due to its excellent mechanical properties, ease of being transformed into fibers, high melting point, non-toxicity, and high chemical stability [18]. This polymer was often mixed with other materials to improve their general performance. In particular, it was used to realize mixtures or composites [19]. PMMA was one polymer often used in association with PAN [20]. Both were immiscible with each other despite being soluble in the same solvent, and this peculiar property had been the subject of various studies, as it allowed the obtention of materials with unique characteristics. Different behaviors of this association were investigated, and some important differences were found, starting from the quantitative ratio used. In general, the arrangement they assumed during the electrospinning process was observed where the PMMA, being heavier, tended to remain compact in the internal part of the fiber, while the PAN, lighter, remained in the external part, covering the whole.

This organization meant that the two polymers, driven by the volumetric pump, remained present as the only continuous structures throughout the process up to the deposit on the collector. The variation of their proportions in the mixture, as well as the solubilization times, the molecular weight, and the average length of the polymers, ensured a great variety of products, characterized by different morphologies and dimensions of the fibers and more or less homogeneous distributions of the same polymers. It was possible to observe how these modifications could create problems during the electrospinning process and produce poor materials for electrospinning. PMMA increased the viscosity of the

polymer solution and became the decisive phase for the creation of the right blend to be electrospun. Furthermore, if in incorrect quantities or in excess, it gave rise to agglomerates and products filled with drops or jets.

PAN and PMMA mixtures in a different ratio were often made as a reaction intermediate for making porous carbon or functionalized material after optimized treatment in various gaseous environments. These two polymers showed different behaviors in different temperatures and the ability to exploit this difference in calcination, lower for PMMA and higher for PAN; in this way, it was possible to obtain a material with variable porosity.

During the pre-oxidation phase, in addition to the structural modification of the PMMA, which mainly degraded into CO₂, there was a structural modification of the PAN which, in an organized manner, began to modify its chemical structure, assuming different conformations. This phase therefore becomes of fundamental importance because we have the first important changes to the sample [21–28].

The reported study focused on the synthesis and characterization of electrospun nanofibers as sorbents for use in the solid-phase extraction of fluoroquinolones and their determination by UHPLC-PDA in human plasma.

In particular, the membrane was obtained starting from a quantity of polymer in a 5:1 ratio of PAN and PMMA stabilized in air at a temperature of 280 °C for about 1 h.

The variables affecting the SPE, such as the amount of adsorbent material, the adsorption time, the ionic strength, the desorption solvent, and the pH of the sample, were investigated. The results show that electrospun nanofibers are very promising and well-performing materials to be used as sorbent. Finally, the possibility of synthesizing fibers of different nature by changing the electrospinning conditions and the polymers used opens a new scenario in the field of adsorbent materials for SPE.

2. Materials and Methods

2.1. Chemicals and Materials

Polyacrylonitrile (PAN, average Mw 150,000), Poly (methyl methacrylate) (PMMA, average Mw 120,000), and Dimethylformamide anhydrous (DMF, 99.8%) were purchased from Sigma-Aldrich. Ciprofloxacin, levofloxacin, lomefloxacin, sparfloxacin, sarafloxacin, gatifloxacin, enrofloxacin, danofloxacin, and ulifloxacin, used as the internal standard (I.S.), were purchased from Santa Cruz Biotechnologies (Dallas, TX, USA). All the analytes had purities better than 98%. Acetonitrile (ACN), methanol (MeOH), hydrochloric acid, triethylamine, and ammonium acetate were provided from Carlo Erba Reagents (Milan, Italy). Ultrapure water was obtained by using a Milli-Q system from Millipore (Bedford, MA, USA). All chemicals used in this work were of the reagent grade.

2.2. Apparatus and UHPLC Conditions

An ultra-high-performance liquid chromatography system (ACQUITY H-Class), equipped with an Acquity UPLC sample manager, a quaternary pump, a column heater, a degassing system, and a photodiode array detector (Waters 2996), was used for the FLQ separation and quantification. Chromatographic separation was achieved using a CORTECS C18 column (75 × 2.1 mm, 2.7 μm) protected by a precolumn (5 × 2.1 mm). The mobile phase consisted of 10 mM ammonium acetate (phase A) adjusted at pH 4.0 with acetic acid and a mixture of acetonitrile/methanol (80/20 *v/v*, phase B); both phases were added with 0.1% *v/v* of triethylamine. Gradient elution was used for the separation of FLQs. The percentage of phase B started from 5% and became 20% in 5 min, then returned to 5% in 0.5 min followed by 1.5 min of column re-equilibration. The flow rate was 0.7 mL/min. Total run time was 7 min. Empower 3.0 (Waters) was used for data collection and for setting up the analysis. Each analyte was determined at its maximum wavelength.

A centrifuge Eppendorf model 5804 R from Eppendorf (Austria) was used for centrifuging the samples. A XS104 Mettler Toledo analytical balance was used to weigh the analytes for the preparation of stock solution and calibration standard.

A syringe pump for infusion model KDSscientific200CE and an electric potential generator model Spellman CZE1000R were used for electrospinning the polymeric solutions. A ball mill model PM1000 was used to reduce the membranes into very small and homogeneous fragments.

2.3. Preparation of Standard Solutions and Real Samples

The stock solutions of FLQs were prepared independently from the QC samples. A total of 20 mg of each reference powder was weighed then transferred into a 10 mL volumetric flask and dissolved with methanol. Working solution of FLQs were obtained by further dilution of stock solutions. A blank human plasma sample (drug-free) was purchased from Sigma-Aldrich. Blood samples, usually taken in the morning from patients at “S.S. Annunziata” Hospital (Chieti, Italy) at the same time as routine TDM samples for plasma, were stored in glass tubes containing EDTA as an anticoagulant. The plasma was obtained by centrifugation at 1300 rpm for 10 min and stored at $-20\text{ }^{\circ}\text{C}$.

2.4. Preparation of PAN Electrospun Nanofibers

After acquiring a straw-yellow color, the solution was left at room temperature for 30 min and then electrospun using a home-made electrospinning system already described in a previous work [29]. PAN and PMMA were dispersed in a 5:1 ratio in DMF and magnetic stirred for 20 h at $60\text{ }^{\circ}\text{C}$ and then for 1 h at room temperature. The solution was fed through the needle of a glass syringe (18 gauge) by a syringe pump for infusion at a constant flow rate of $0.70\text{--}0.80\text{ mL h}^{-1}$ applying a DC voltage between 13 and 16 kV. The distance between the needle and the collector ($10 \times 10\text{ cm}$ stainless steel covered with aluminium foil) was 18 cm. The temperature and the relative humidity were $28\text{ }^{\circ}\text{C}$ and 36%, respectively. The polarity of the electric field was set and directed from positive to negative charge. The electrospun membranes were stabilized in air at $280\text{ }^{\circ}\text{C}$ for 1 h. Finally, the electrospun polymers were ground (to simplify the packing step in SPE cartridges) for 45 min at 250 rpm alternating 5 min of pause after 5 min of stirring using a ball mill (model PM1000, Retsch GmbH, Haan, Germany) to reduce the membranes into small and homogeneous fragments.

2.5. Solid-Phase Extraction Procedure

The SPE cartridges were previously emptied and packed with 45 mg of sorbent. Cartridges were conditioned with $2 \times 1\text{ mL}$ of methanol followed by $2 \times 1\text{ mL}$ of sodium acetate buffer 10 mM (pH 5). Samples or blank plasma spiked with FLQs were loaded onto conditioned cartridges using Visiprep 12 solid-phase Extraction Vacuum Manifold. After the loading step, samples were washed with 1 mL sodium acetate buffer 10 mM (pH 5) to eliminate the interferences and eluted with 1 mL of methanol, which was subsequently evaporated to dryness under a nitrogen stream using a drying attachment apparatus at room temperature and re-constituted with 100 μL of a mixture of water and methanol (50/50 *v/v*). The solution was further filtered on Phenex-PTFE (4 mm, $0.45\text{ }\mu\text{m}$) filters, and finally, 5 μL was injected into the UHPLC system.

2.6. Characterization

Rheological analysis (viscosity profile) of the PAN-PMMA blend was evaluated using a Rheometer MCR 102 (Anton Paar, Graz, Austria). The flow curve was generated increasing the shear rate ($\dot{\gamma}$) linearly and stepwise between 0.1 and 100 s^{-1} . The resulting flow curve was fitted with a Herschel–Bulkley regression model.

The surface morphology of the PAN-PMMA electrospun fibers was observed by using a MultiMode 8 AFM microscope with Nanoscope V controller (Bruker, Billerica, MA, USA). The sample was scanned by the silicon ScanAsyst-Air probe (triangular geometry, cantilever resonance frequency 70 KHz and nominal spring constant 0.4 N/m) at a 0.535 Hz scan rate with ScanAsyst auto control. Images of 512×512 pixels were collected with scan sizes of

10 $\mu\text{m} \times 10 \mu\text{m}$ and were elaborated with NanoScope Analysis 1.8 software to analyze the surface roughness and the fiber diameter.

To complete the morphological study, SEM images were acquired using the Phenom XL Desktop apparatus, obtained in backscatter mode at 1 Pa high vacuum with an optical magnification of 1000 \times , 2500 \times and 20,000 \times , respectively, and an acceleration voltage of 15 KV. The Phenom ProSuite software was used for the elemental analysis, the atomic distribution, and the size measurement information. The Electron Microscopy Sciences SEM K550 was used to sputter each sample with a thin layer of gold.

Fourier transform infrared (FTIR) spectra were acquired in triplicate using a Shimadzu IRAffinity-1S FTIR spectrophotometer in a range from 3250 to 450 cm^{-1} . LabSolution IR version 2.27 was the software used for the spectra manipulation.

A PerkinElmer STA6000 with Pyris software was used for the thermogravimetric analyses. Each sample was heated in an atmosphere environment with a flow of 20 mL/min at a rate of 10 $^{\circ}\text{C}/\text{min}$ to 950 $^{\circ}\text{C}$ with a final isotherm of 15 min.

Brunauer Emmett Teller (BET) analyses were acquired across nitrogen adsorption isotherms at 77 k using the Micromeritics ASAP 2020 Plus Adsorption Analyzer. For each analysis, the sample was degassed at a temperature of 120 $^{\circ}\text{C}$ for 12 h under ultra-high vacuum. Relative pressure points P/P_0 in the range 0.0001–0.01 were included to evaluate the extent of possible microporosity, and the BET surface area was calculated over the nominal pressure range between 0.05–0.25. The BJH model was used to calculate the pore size and volume distribution up to 200 nm.

3. Results and Discussion

3.1. Characterization of Electrospun Nanofibers

A 5:1 ratio of PAN:PMMA was used to prepare the polymer blend to be electrospun. Its viscosity was measured to evaluate possible electrospinnability [28]. Figure 1 shows the graphical representation of the main steps of the work.

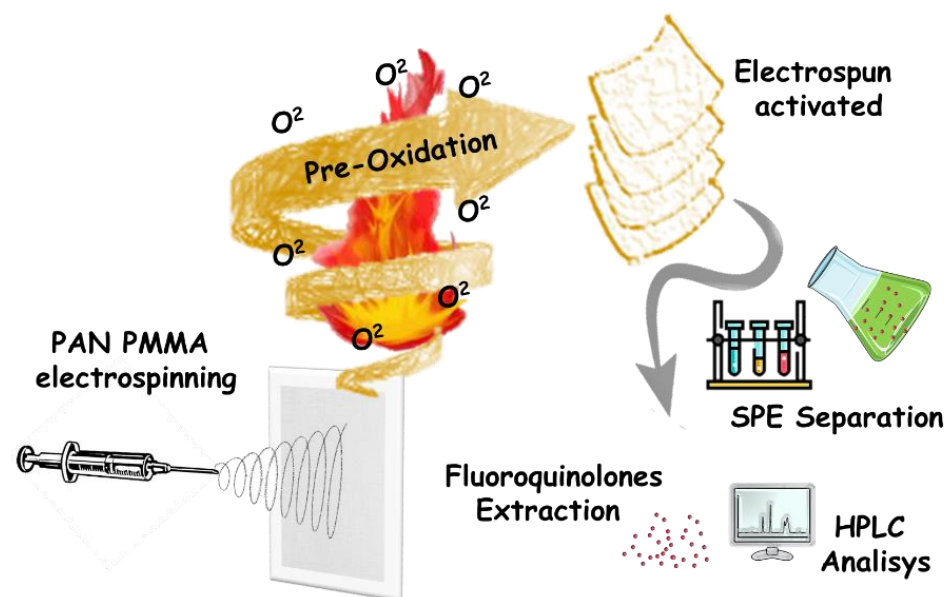


Figure 1. Graphical representation of the main steps of sample preparation.

The two mixed polymers were distributed in an organized manner within the same solution, presenting a certain viscosity value and a straw-yellow color. This blend solution demonstrates a Newtonian behavior. Figure 2 highlights the relation between the shear stress (τ) and viscosity (η) at various shear rates ($\dot{\gamma}$). The resulting curves are typical of “liquid-like” materials showing a constant η and a τ that increases in the range of the considered $\dot{\gamma}$. These results reveal that, at a constant temperature, the η is independent

from the applied velocity gradient. The Herschel–Bulkley model, guaranteeing the best fitting, was proposed to predict the η , the result of which was 44.77 mPa·s [30].

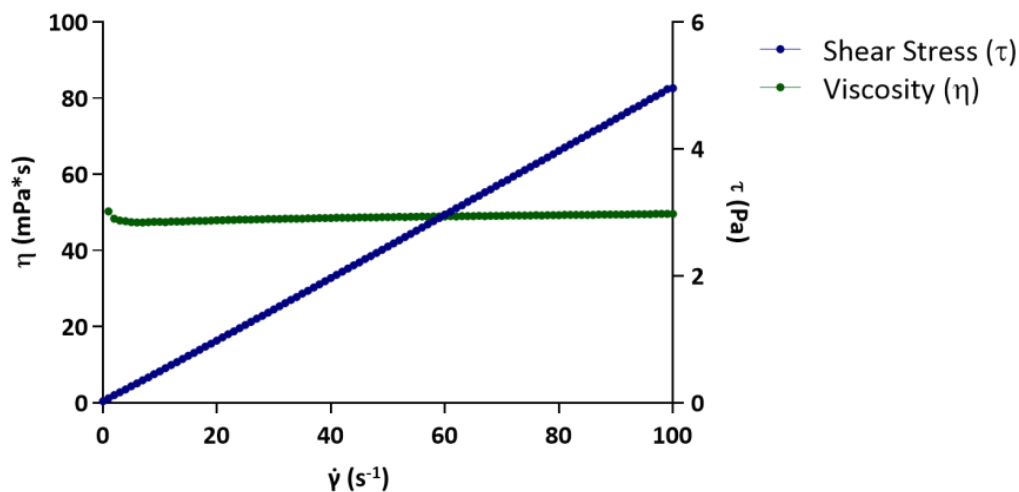


Figure 2. Newtonian flow of PAN-PMMA blend solution.

The morphology of the PAN-PMMA 5:1 ratio electrospun fibers was further studied by AFM, analyzing the sample without any surface coating. In Figure 3 are shown the AFM height channels of fibers in 2D and 3D representations. The analyzed sample revealed a randomly oriented three-dimensional structure with homogeneous cylinder-like fiber geometry. The PAN-PMMA average fiber diameter, calculated by cross-section measurements taken from different sample images, was 328 ± 55 nm. The average image roughness (R_a) and the root mean square of the surface roughness (R_q) were found to be 556 ± 15 nm and 680 ± 16 nm, respectively, considering that the fibers covered 93% of the image surface area.

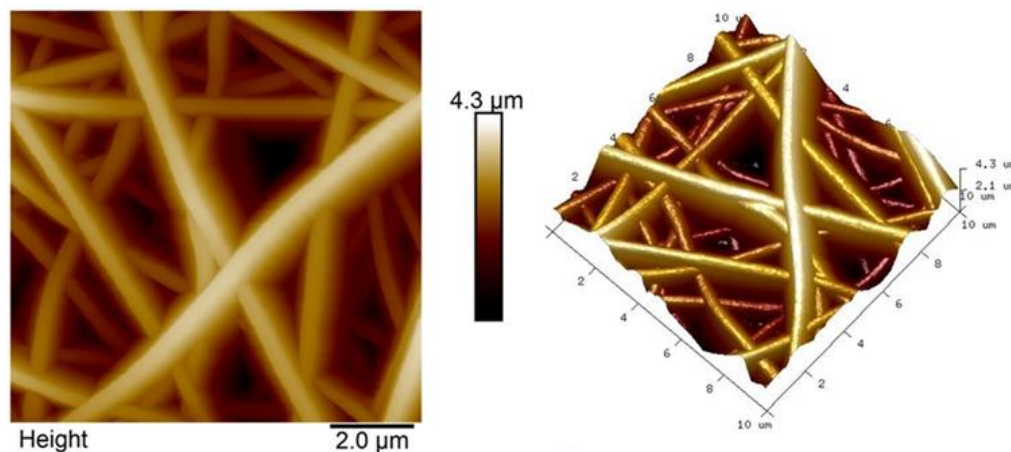


Figure 3. AFM images of 2D and 3D surface topography of PAN-PMMA electrospun fibers.

In Figure 4, the SEM images are shown. The dimensions of the fibers and their random and homogeneous distribution were confirmed. Magnifications were made to $1000\times$, $2500\times$, and $20,000\times$, respectively, to better evaluate the random distribution of the fibers and the possible roughness of the single filament. It was possible to observe how there were no fused portions and how each fiber maintained its own constant and homogeneous shape along its entire length. A small layer of gold had to be deposited to increase resolution and avoid overheating of the sample.

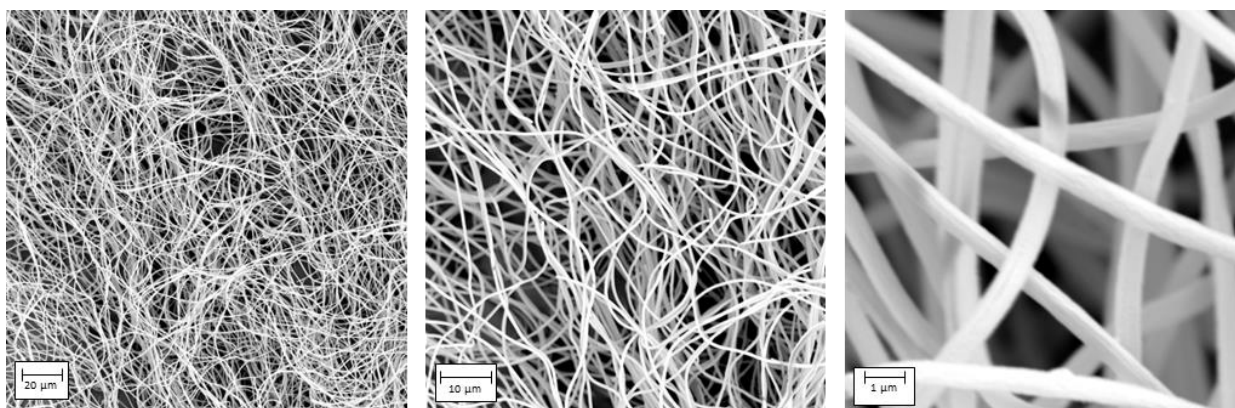


Figure 4. SEM images of PAN-PMMA fibers at magnifications of 1000×, 2500×, and 20,000×, respectively.

Through the Phenom ProSuite software, it was possible to observe the distribution of the various atoms in the material. In Figure 5, it is possible to observe a sample where the carbon atoms, colored in red, the nitrogen, colored in green, and the oxygen, colored in purple, were present in a very homogeneous way.

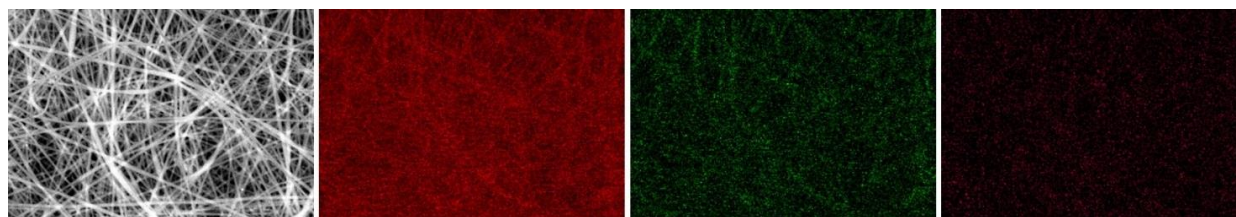


Figure 5. SEM-EDX images of PAN-PMMA fibers. The distribution of carbon atoms (in red), nitrogen (in green), and oxygen (in purple) is shown.

In Figure 6 showing the FTIR spectra, the distinct presence of the two polymers used was confirmed. In particular, two characteristic peaks were observed, the first relating to the absorption band of the carbonyl stretching at 1730 cm^{-1} and the second to the stretching of the acrylonitrile unit assigned to the $\text{-C}\equiv\text{N}$ bond at 2243 cm^{-1} , typical of PMMA and PAN, respectively.

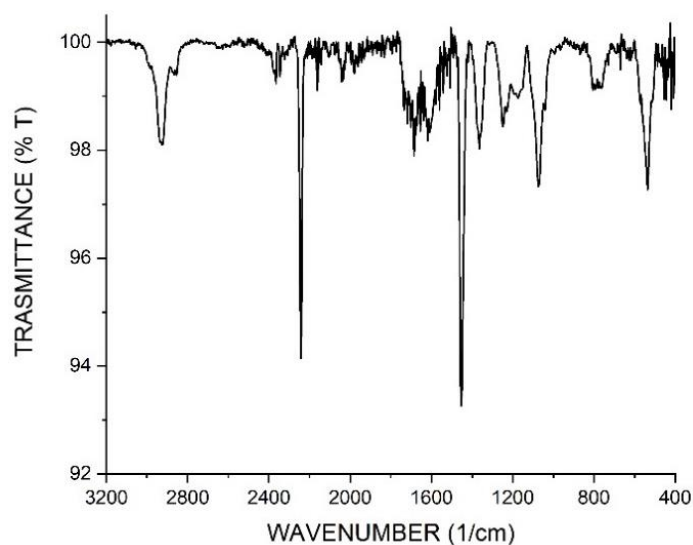


Figure 6. FTIR analysis of PAN-PMMA electrospun membrane.

The peaks relating to PAN are more clearly observable as this was present in greater quantities than PMMA. Indeed, the peak of greatest intensity was correlated to that of PAN [31,32].

It was also possible to observe the peaks relating to the stretching, bending, and twisting of the CH₂ bond at 2924 and 2854 cm⁻¹ and at 1452 cm⁻¹ and 1247 cm⁻¹, respectively.

From Figure 7, it is possible to observe the thermal degradation of the PAN-PMMA electrospun membrane. There was an initial weight loss at about 100 °C due to water loss. A slow stabilization of the entire sample followed up to a temperature of 300 °C, where the PMMA began to decompose, losing part of its characterizing groups, such as CO₂, and the PAN began the cyclization of the nitrile groups and the dehydrogenation [33–35].

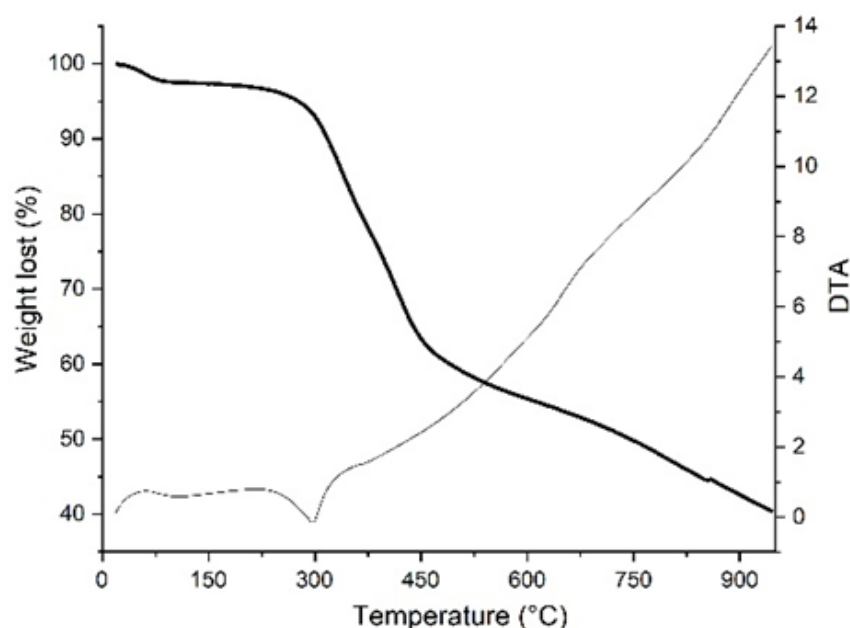


Figure 7. TGA and DTA analysis of PAN-PMMA electrospun membrane.

From 300 °C to 450 °C, the degradation kinetics were fast due to the complete degradation of PMMA. Above 450 °C, the degradation kinetics were slower and peculiarly correlated to the dehydrogenation and denitrogenation of PAN. The residue that is obtained by calcining up to a temperature of 950 °C resulted in a porous carbon with a yield of about 40%.

BET analyses showed a very high surface area and porosity, as reported in Figure 8. Furthermore, the data obtained from the t-Plot of the external surface and from the BJH Absorption/Desorption described the presence of a good homogeneity of the whole structure. Of importance was the nanometric size of the pores, well-distributed and easily accessible over the entire surface. There were observed Type-4-like nitrogen adsorption–desorption isotherms with an apparent hysteresis between the two curves. The shape of the isotherms' adsorption indicated a small content of micropores and a significant content of mesopores, confirmed by the presence of the hysteresis loop. With the BJH method it was possible to observe in Figure 7 the presence of small pores with values between 1.7 and 25 nm. The apparent surface areas calculated in a range from 0.05 to 0.25 of relative pressure (P/P₀) were 659.16 m² g⁻¹ (Figure 8b). The points were fitted using a first-degree linear equation:

$$y = a + b * x$$

with an intercept of $0.00241 \pm 3.90523 \times 10^{-6}$, a slope of $0.0042 \pm 2.92391 \times 10^{-5}$, and a Adj. R-Square of 0.99961.

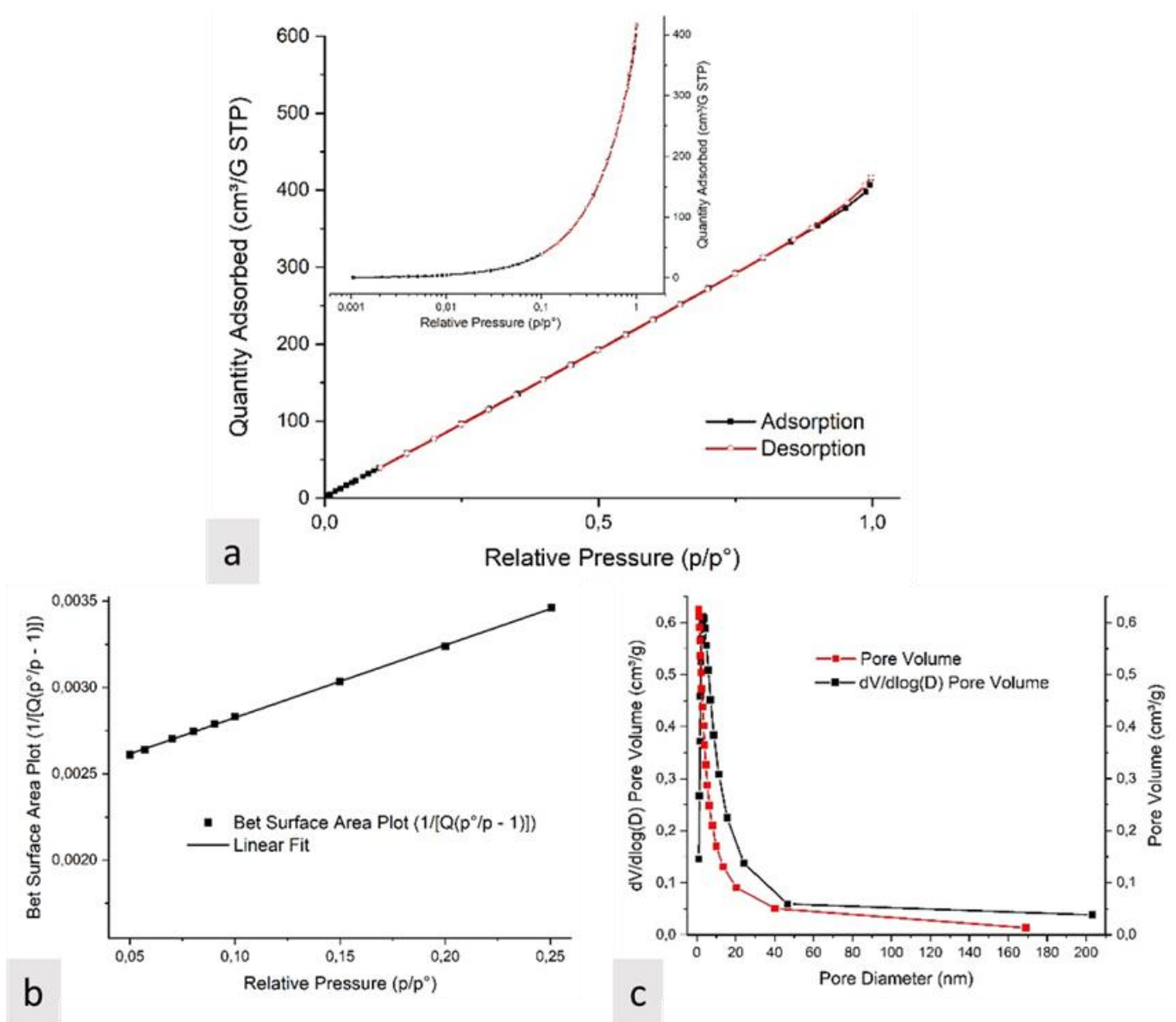


Figure 8. (a) Isotherms of nitrogen adsorption at 77 K (logarithmic plot in the inset); (b) BET surface area plot; (c) pore size distribution (BJH model).

3.2. Optimization of the Extraction Procedure

The variables which influence the solid-phase extraction of FLQs in human plasma were evaluated by studying the effect of one variable at a time and using recovery as a response. Recovery was evaluated comparing the analyte to I.S. ratios in extracted spiked plasma sample to extracted blank plasma sample spiked post-extraction at the same concentration. Standard solutions containing FLQs at the concentration of 1 µg/mL were used for those experiments. In this study, the parameters affecting the adsorption (amount of sorbent and pH of the sample) and the desorption (type of eluent and its volume) were investigated.

3.2.1. Effect of the pH

The sample pH is a fundamental parameter for the success of the extraction. In this study, to evaluate and optimize the sample pH during the loading step, experiments were performed at different sample pH (2.5–10). As reported in Figure 9, an increase in the recovery was obtained starting from pH 2.5 to pH 5, while a decrease in recovery is obtained using solutions at pH 7.5 and 10. As further proof of the adsorption of the analytes on the

cartridge, the eluate obtained in the loading step was analyzed in UHPLC-PDA. No signals attributable to FLQs were observed using a pH 5 solution, while signals of several FLQs were observed when other pH values were used.

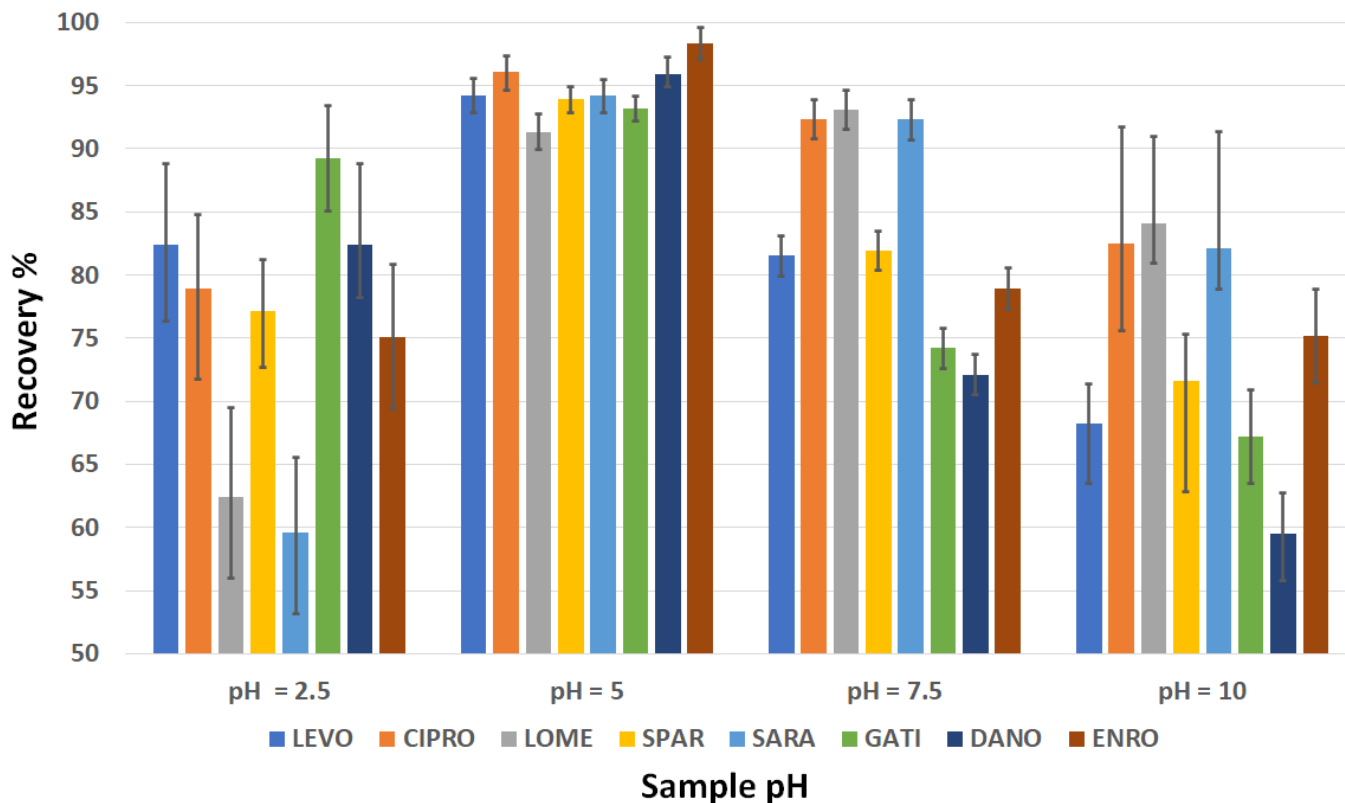


Figure 9. Effect of sample pH (x-axis) on the recovery (y-axis) of FLQs.

3.2.2. Effect of PAN-PMMA Nanofiber Amount and Sample Volume

The amount of PAN-PMMA nanofiber was investigated to maximize extraction efficiency in the range of 15–90 mg. The extraction efficiency increases as the quantity of PAN-PMMA nanofiber increases up to 45 mg, after which it remains almost constant, as shown in Figure 10. Consequently, 45 mg was chosen as the quantity of sorbent to be used for further experiments, since 45 mg of sorbent are sufficient for the complete adsorption of FLQs. This is due to the chemical and physical characteristics of the nanofibers which allow the obtention, compared with other sorbents, of identical or better results using a smaller quantity of sorbent. It is obvious that increasing the quantity of sorbent would increase the accessible sites for the adsorption of the analytes; however, difficulties would be encountered in the elution step, as the desorption ability of the eluent could be insufficient for the complete elution of the analytes.

The sample volume to be used was tested by extracting different volumes (1 to 10 mL) of blank plasma spiked with FLQs and keeping their masses constant in all cases. From the results obtained, it was noted that by increasing the sample volume from 1 to 3 mL, it is possible to obtain a slight increase in recoveries, while volumes greater than 3 mL drastically reduce recoveries.

This result can be explained by the fact that human plasma is a matrix containing many interferents that could compete with the analytes, causing the saturation of the active sites present on the surface of the sorbent.

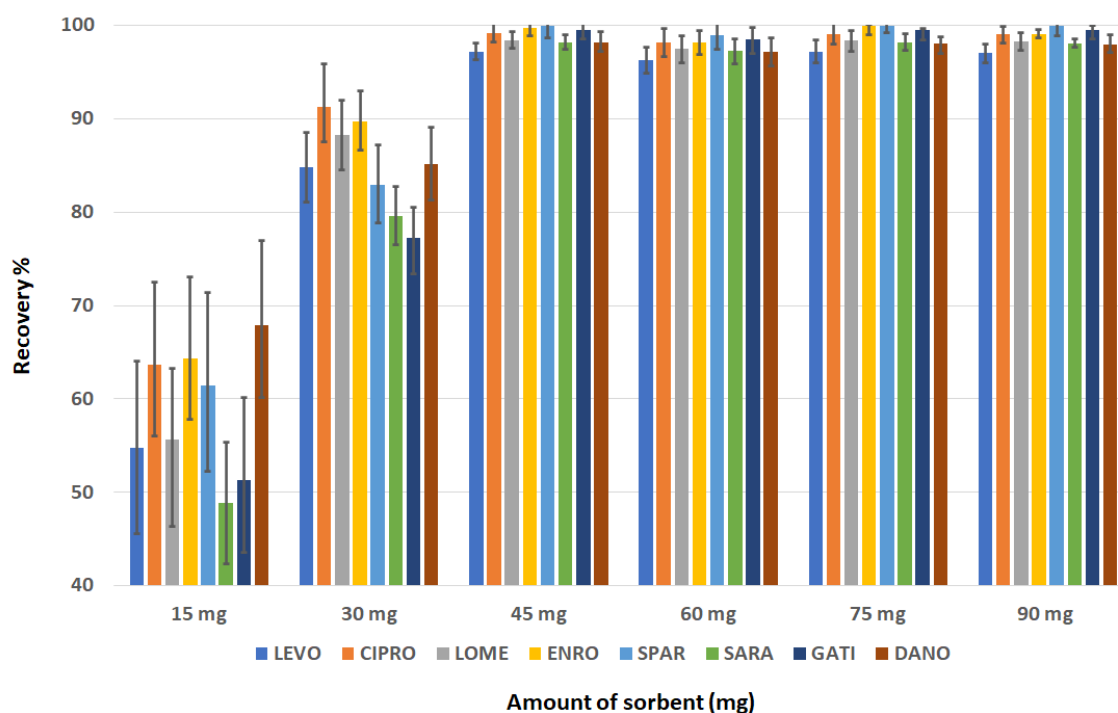


Figure 10. Effect of sorbent amount on the recovery.

3.2.3. Effect of Washing Solution

To evaluate the effects of the washing solution on analyte retention and to minimize its loss in the washing step, different washing solutions were tested. The first solution tested was ultrapure water alone and a solution containing water and methanol (90:10 *v/v*). It was observed that the water alone allows sufficient removal, but at the same time, it involves a small loss in the recoveries, while the solution containing water and methanol allowed the obtention of an excellent cleaning of the extract from the interferents, but at the same time provided an unsatisfactory recovery. Finally, taking into account the results reported in Figure 8, a sodium acetate buffer at pH 5 was tested as a washing solvent, obtaining as a result a clean chromatogram and no loss of analytes. The use of a buffered solution of sodium acetate at pH 5 and methanol (90:10 *v/v*) resulted in decreased recoveries of FLQs. For this reason, 1 mL of sodium acetate buffer pH 5 was used as washing solution.

3.2.4. Effect of Elution Solvent Type and Volume

To evaluate the most suitable solvent for the elution of FLQs from SPE cartridges, several organic solvents were tested, including methanol, acetonitrile, and isopropanol. Among these solvents, the best performances were obtained using methanol. Furthermore, the volumes of methanol to be used to ensure the complete elution of the FLQs were evaluated in the range of 250–1500 μL . The results obtained showed 1000 μL to be sufficient and to guarantee a high reproducibility. Volumes lower than 1000 μL are insufficient for the complete elution of all FLQs and lead to poor reproducibility, while higher volumes lead to no benefit. For these reasons, 1000 μL of methanol was used for the elution of the FLQs for the proposed method.

3.3. Analytical Performance of the Proposed SPE Method

The proposed method was validated according to the FDA guidelines [36]. Selectivity of the method was tested by extracting six different sources of blank matrix. Chromatographic analysis of the blank matrices showed no interference between the endogenous compounds and the analytes at their retention times, as reported in Figure 11.

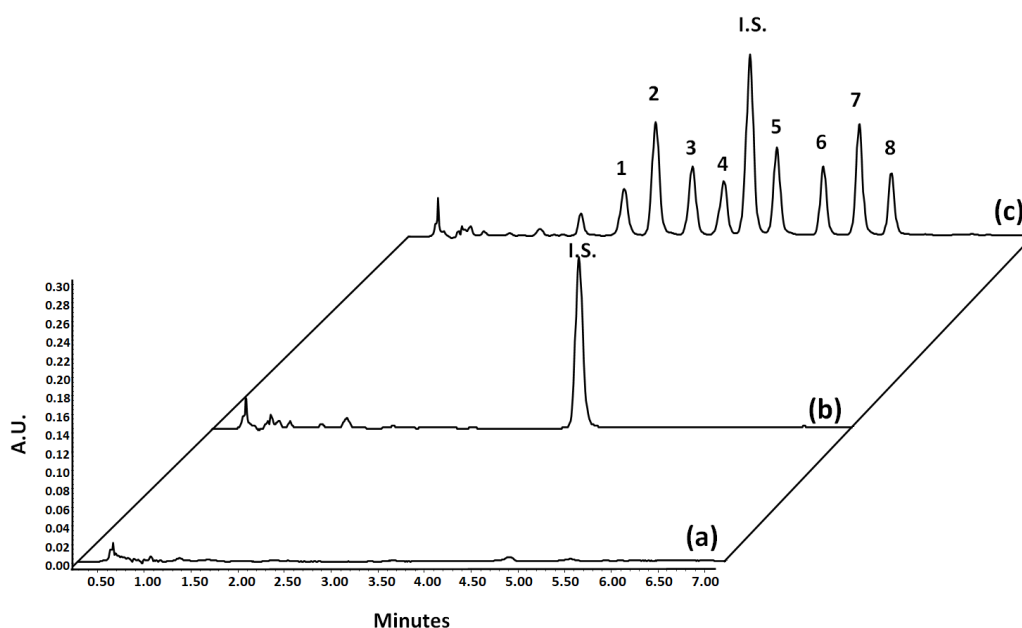


Figure 11. UHPLC chromatograms of blank plasma extracted (a), blank plasma spiked with I.S. extracted (b), blank plasma spiked with levofloxacin (1), lomefloxacin (2), enrofloxacin (3), ciprofloxacin (4), gatifloxacin (5), sparfloxacin (6), sarafloxacin (7), and danofloxacin (8), and the I.S. extracted (c).

Furthermore, the analytes were well resolved. A calibration curve for each FLQ was constructed in the range of 10–0.005 µg/mL using a least squares linear regression. A calibration curve was constructed for each FLQ in the range 10–0.005 µg/mL using a linear least squares regression, with concentration as the independent variable and the analyte/internal standard peaks area ratio as the dependent variable. Statistical analysis of concentration/response relationships demonstrated that a linear correlation was the best model, with a mean correlation coefficient (r^2) > 0.9993. Signal-to-noise ratios of 1:3 and 1:10 were used to evaluate limits of detection (LOD) and quantification (LOQ), respectively. For the proposed method, LOQs were 0.005 and LODs 0.001 µg/mL, respectively, for all the FLQs investigated. Precision and accuracy were assessed by the analysis of three batches of quality control samples (QCs) at three concentrations in triplicate and for five consecutive days ($n = 5$), as shown in Table 1. These results satisfy the limits imposed by the guidelines, because for the proposed SPE-UHPLC-PDA method, the precision, expressed as relative standard deviation percentage (RSD%), is below 5.2% and the accuracy, expressed as BIAS%, is between −6.2% and 3.8%. Recovery was evaluated spiking blank samples with FLQs and comparing the ratio of spiked blank extract to standard solution at the same concentration. Moreover, as further proof of the adsorption, after the loading phase in SPE, the eluate was analyzed to verify the absence of FLQs and demonstrate the effective adsorption of the analytes on the sorbent.

Table 1. Precision and accuracy of the proposed SPE-UHPLC-PDA method.

Analyte	Concentration	Precision		Accuracy	
		Intra-Day	Inter-Day	Intra-Day	Inter-Day
Levofloxacin	LLOQ	4.9	5.1	+5.1	+6.3
	QCL	3.5	3.8	+4.9	+5.5
	QCM	4.7	5.0	−2.0	−4.7
	QCH	2.3	1.9	−1.1	−3.2
Ciprofloxacin	LLOQ	4.9	5.0	−1.9	−3.2
	QCL	3.1	3.9	+1.5	+1.9
	QCM	4.1	4.4	−4.0	−5.3

Table 1. *Cont.*

Analyte	Concentration	Precision		Accuracy	
		Intra-Day	Inter-Day	Intra-Day	Inter-Day
Lomefloxacin	QCH	4.4	3.9	+5.3	+6.0
	LLOQ	5.0	4.9	+7.0	+7.4
	QCL	1.2	3.0	−6.4	−6.8
	QCM	2.3	3.0	−5.9	−5.9
	QCH	2.2	2.2	+3.1	+3.2
Enrofloxacin	LLOQ	4.8	5.0	+5.9	+6.9
	QCL	2.2	2.5	+0.7	+2.1
	QCM	1.8	2.4	+0.2	+1.0
	QCH	3.1	2.3	−4.2	−5.5
Sparfloxacin	LLOQ	5.0	4.9	−0.9	−1.5
	QCL	2.6	2.7	+3.1	+3.6
	QCM	0.9	1.7	+6.5	+6.1
	QCH	1.1	2.0	−3.2	−3.3
Sarafloxacin	LLOQ	4.7	3.3	−4.4	−5.9
	QCL	3.1	3.9	+3.2	+3.6
	QCM	2.3	3.1	+1.1	+1.9
	QCH	1.5	4.0	+4.2	+4.0
Gatifloxacin	LLOQ	4.0	5.1	−3.1	−3.4
	QCL	2.2	4.0	+2.7	+3.6
	QCM	2.4	3.3	+4.8	+5.9
	QCH	1.4	3.0	+6.5	+6.0
Danofloxacin	LLOQ	3.9	3.5	−6.1	−5.4
	QCL	3.0	4.9	−5.4	−6.0
	QCM	1.5	3.1	+2.6	+3.1
	QCH	2.0	4.0	+0.3	+0.9

3.4. Comparison with Existing Method in Literature

Fluoroquinolones are analytes that have been extensively researched; as a result, there are numerous methods today for their determination and quantification. Among sample preparation methods used, the most used are those involving interaction with a sorbent; this is because solid-phase extraction or sorbent-based methods offer greater reproducibility and because in recent years, more and more new materials capable of offering performances clearly superior to those offered by traditional solvents in the LLE have been developed. Different methods for the determination of fluoroquinolones from different matrices are reported in Table 2. The prepared electrospun material, used as an adsorbent material in SPE cartridges, was compared with the methods reported in the literature. From the comparison it is evident that the proposed method has limits of quantification comparable or even higher than the methods reported. In addition, ultra-high-performance liquid chromatography offers the possibility of significantly reducing analysis times. Accordingly, the proposed solid-phase extraction method based on using electrospun materials as sorbents can be used in the determination of fluoroquinolones.

Table 2. Comparison of the proposed method with methods present in literature.

Analyte	Matrix	Sample Preparation	Instrumentation	Range (µg/mL)	Mean Recovery	LOQ (µg/mL)	Ref.
CIP, MOX ^a , LEV, ULI	Human plasma	MEPS ^b	HPLC-PDA	0.1–10	n.a.	0.1	[37]

Table 2. Cont.

Analyte	Matrix	Sample Preparation	Instrumentation	Range (µg/mL)	Mean Recovery	LOQ (µg/mL)	Ref.
OFL ^c , CIP	Human plasma	HF-LPME ^d	HPLC-UV	0.01–5	30%	0.01	[38]
MAR ^e , LOM, DIF ^g , NOR ^h , CIP, ENR	Milk	dMSPE ^f	HPLC-PDA	0.01–20	94.7%	0.01	[39]
CIP, ENR, SAR, DIF, DAN	Water, Egg, Milk	SPE	UHPLC-FLD	0.005–10	101.9%	0.005	[40]
OFL, ENR, DAN	Milk	dMSPE	HPLC-UV	0.05–1.0	80.1%	0.05	[41]
FLE ⁱ , GAT, LOM, NOR	Milk	dMSPE	CE ^j -UV	0.03–1.0	102.1%	0.03	[42]
CIP, LEV, LOM, SPA, SAR, GAT, ENR, DAN	Human plasma	SPE	UHPLC-PDA	0.005–10	98.9%	0.005	This work

^a: moxifloxacin; ^b: Micro-extraction by packed sorbent; ^c: Ofloxacin; ^d: Hollow-fiber liquid-phase micro-extraction; ^e: Marbofloxacin; ^f: dispersive magnetic solid phase extraction; ^g: Difloxacin; ^h: Norfloxacin; ⁱ: Fleroxacin; ^j: Capillary electrophoresis.

4. Conclusions

In this study, electrospun PAN PMMA membranes optimized in a 5:1 ratio were studied and characterized for the realization of sorbents for the extraction of fluoroquinolones in plasma samples. The proposed method has its strengths in its simplicity and in its excellent performances, if compared with other methods already present in the literature. Figure 11 shows the graphical representation of the main phases of the work. The combination obtained allowed a good distribution of the two polymers, with PMMA present only in the innermost part of the fiber, which followed one another along its entire length without forming aggregates, which would have disturbed the electrospinning process and PAN in the outermost part. From the characterization carried out, the material appeared uniform and free of beads. Furthermore, the surface area was very large and allowed the separation of many possible areas of interaction with the samples. Activation of the membrane through the pre-oxidation step allowed for greater sample stability and an arrangement of molecular structures containing carbonyl and nitrile groups capable of establishing optimal interactions with any analyte to be observed. Unfortunately, this system did not overcome all the limits present with the methods currently in use, but it had the advantage of being cheap and simple. Even in small quantities of a few milligrams, it has proved to perform well in various working conditions.

Author Contributions: Conceptualization, V.F. and P.B.; methodology, V.F. and P.B.; software, P.B. and E.M.; validation, V.F. and P.A.; formal analysis, P.D.P., L.M., S.P. and L.S.; investigation, V.F., P.B., L.M., L.S. and S.P.; resources G.C. and S.F.; data curation, V.F., P.B. and E.M.; writing—original draft preparation, V.F. and P.B.; writing—review and editing, G.C. and S.F.; visualization, V.F. and P.B.; supervision, G.C., S.F. and P.D.P.; project administration, G.C.; funding acquisition, P.B. and S.F. All authors have read and agreed to the published version of the manuscript.

Funding: P.B. received funding for his post by MUR (Ministry for Universities and Research) under the act PON “Ricerca e Innovazione” 2014–2020 “Linea di Attività: Azioni IV.6 Green—contratti di ricerca su tematiche ‘Green’—D.M. 1062 del 10/08/2021” grant number ‘CUP D55F210030800050’.

Informed Consent Statement: Informed consent was obtained from all subjects involved in the study.

Data Availability Statement: The data presented in this study are available on request from the corresponding author.

Acknowledgments: The authors would like to thank Francesco Nobili, Antonio Di Stefano, Francesco Stoppa, Antonella Fontana, and Gianluigi Rosatelli for making part of their equipment available (TGA, BET, Rheometer and SEM-EDX).

Conflicts of Interest: The authors declare no conflict of interest.

References

1. Carlucci, G. Analysis of fluoroquinolones in biological fluids by high performance liquid chromatography: Review. *J. Chromatogr. A* **1998**, *812*, 343–367. [[CrossRef](#)]
2. Lipsky, B.A.; Baker, C.A. Fluoroquinolone Toxicity Profiles: A Review Focusing on Newer Agents. *Clin. Infect. Dis.* **1999**, *28*, 352–364. [[CrossRef](#)] [[PubMed](#)]
3. Kamberi, M. Pharmacokinetic/Pharmacodynamic Parameters: Rationale for Antibacterial Dosing of Mice and Men. *Clin. Infect. Dis.* **1998**, *26*, 1–12.
4. Hooper, D.C. Mechanisms of action and resistance of older and newer fluoroquinolones. *Clin. Infect. Dis.* **2000**, *31*, S24–S28. [[CrossRef](#)] [[PubMed](#)]
5. Chen, Y.; Guo, Z.; Wang, X.; Qiu, C. Sample preparation. *J. Chromatogr. A* **2008**, *1184*, 191–219. [[CrossRef](#)] [[PubMed](#)]
6. Moldoveanu, S.C.; David, V. *Sample Preparation in Chromatography*; Elsevier: Amsterdam, The Netherlands, 2002.
7. Buszewsky, B.; Szultka, M. Past, present and future of solid phase extraction: A review. *Crit. Rev. Anal. Chem.* **2012**, *42*, 198–213. [[CrossRef](#)]
8. Ferrone, V.; Todaro, S.; Carlucci, M.; Fontana, A.; Ventrella, A.; Carlucci, G.; Milanetti, E. Optimization by response surface methodology of a dispersive magnetic solid phase extraction exploiting magnetic graphene nanocomposite coupled with UHPLC-PDA for simultaneous determination of new oral anticoagulants (NAOs) in human plasma. *J. Pharm. Biomed. Anal.* **2020**, *179*, 112992. [[CrossRef](#)]
9. Ferrone, V.; Carlucci, M.; Palumbo, P.; Carlucci, G. Bioanalytical method development for quantification of ulifloxacin, fenbufen and felbinac in rat plasma by solid-phase extraction (SPE) and HPLC with PDA detection. *J. Pharm. Biomed. Anal.* **2016**, *123*, 205–212. [[CrossRef](#)]
10. Pawliszyn, J.; Lord, H.L. *Handbook of Sample Preparation*; Wiley: New York, NY, USA, 2010.
11. Milanetti, E.; Carlucci, G.; Olimpieri, P.P.; Palumbo, P.; Carlucci, M.; Ferrone, V. Correlation analysis based on the hydrophobic properties of non-steroidal anti-inflammatory drugs in solid-phase extraction (SPE) and reversed-phase high performance liquid chromatography (HPLC) with photodiode array detection and their applications to biological samples. *J. Chromatogr. A* **2019**, *1605*, 3603351.
12. Casado, N.; Gañán, J.; Zarcero, S.; Sierra, I. New Advanced Materials and Sorbent-Based Microextraction Techniques as Strategies in Sample Preparation to Improve the Determination of Natural Toxins in Food Samples. *Molecules* **2020**, *25*, 702. [[CrossRef](#)]
13. Nayl, A.; Abd-Elhamid, A.; Awwad, N.; Abdelgawad, M.; Wu, J.; Mo, X.; Gomha, S.; Aly, A.; Bräse, S. Review of the Recent Advances in Electrospun Nanofibers Applications in Water Purification. *Polymers* **2022**, *14*, 1594. [[CrossRef](#)] [[PubMed](#)]
14. Yoshimatsu, K.; YE, L.; Lindberg, J.; Chronakis, I. Selective molecular adsorption using electrospun nanofiber affinity membranes. *Biosens. Bioelectron.* **2008**, *23*, 1208–1215. [[CrossRef](#)] [[PubMed](#)]
15. Xue, J.; Wu, T.; Dai, Y.; Xia, Y. Electrospinning and Electrospun Nanofibers: Methods, Materials, and Applications. *Chem. Rev.* **2019**, *119*, 5298–5415. [[CrossRef](#)] [[PubMed](#)]
16. Luraghi, A.; Peri, F.; Moroni, P. Electrospinning for drug delivery applications: A review. *J. Control. Release* **2021**, *334*, 463–484. [[CrossRef](#)] [[PubMed](#)]
17. Hong, C.; Yang, K.; Oh, S.; Ahn, J.; Cho, B.; Nah, C. Effect of blend composition on the morphology development of electrospun fibers based on PAN/PMMA blends. *Polym. Int.* **2008**, *57*, 1357–1362. [[CrossRef](#)]
18. Wang, T.; Kumar, S. Electrospinning of polyacrylonitrile nanofibers. *J. Appl. Polym. Sci.* **2006**, *102*, 1023–1029. [[CrossRef](#)]
19. Chinchillas, M.; Gaxiola, A.; Beltrán, C.; Orozco, V.; Cervantes, M.; Rodríguez, M.; Beltrán, A. A new application of recycled-PET/PAN composite nanofibers to cement-based materials. *J. Clean. Prod.* **2020**, *252*, 119827. [[CrossRef](#)]
20. Babo, S.; Ferreira, J.L.; Ramos, A.M.; Micheluz, A.; Pamplona, M.; Casimiro, M.H.; Ferreira, L.; Melo, M. Characterization and Long-Term Stability of Historical PMMA: Impact of Additives and Acrylic Sheet Industrial Production Processes. *Polymers* **2020**, *12*, 2198. [[CrossRef](#)]
21. Gopiraman, M.; Kim, I. Preparation, Characterization and Applications of Electrospun Carbon Nanofibers and Its Composites. In *Electrospinning Electro Spray—Techniques and Application*; Intech Open: Rijeka, Croatia, 2019; Chapter 3.
22. Kopec, M.; Lamson, M.; Yuan, R.; Tang, C.; Kruk, M.; Zhong, M.; Matyjaszewski, K.; Kowalewski, T. Polyacrylonitrile-derived nanostructured carbon materials. *Prog. Polym. Sci.* **2019**, *92*, 89–134. [[CrossRef](#)]
23. Choi, S.; Han, E.; Park, K. Porosity Control of Electrospun PAN/PMMA Nanofiber Webs. *Mol. Cryst. Liq. Cryst.* **2019**, *688*, 68–74. [[CrossRef](#)]
24. Abeykoon, N.; Bonso, J.; Ferraris, J. Supercapacitor performance of carbon nanofiber electrodes derived from immiscible PAN/PMMA polymer blends. *RSC Adv.* **2015**, *5*, 19865–19873. [[CrossRef](#)]
25. Bazilevsky, A.; Yarin, A.; Megaridis, C. Co-electrospinning of Core-Shell Fibers Using a Single-Nozzle Technique. *Langmuir* **2007**, *23*, 2311–2314. [[CrossRef](#)] [[PubMed](#)]

26. He, G.; Song, Y.; Chen, S.; Wang, L. Porous carbon nanofiber mats from electrospun polyacrylonitrile/polymethylmethacrylate composite nanofibers for supercapacitor electrode materials. *J. Mater. Sci.* **2018**, *53*, 9721–9730. [[CrossRef](#)]
27. Khanlou, H.M.; Ang, B.C.; Talebian, S.; Afif, A.M.; Andriyana, A. Electrospinning of polymethyl methacrylate nanofibers: Optimization of processing parameters using the Taguchi design of experiments. *Text. Res. J.* **2015**, *85*, 356–368. [[CrossRef](#)]
28. Xuan, D.; Liu, J.; Wang, D.; Lu, Z.; Liu, Q.; Liu, Y.; Li, S.; Zheng, Z. Facile Preparation of Low-Cost and Cross-Linked Carbon Nanofibers Derived from PAN/PMMA/Lignin as Supercapacitor Electrodes. *Energy Fuels* **2021**, *35*, 796–805. [[CrossRef](#)]
29. Maroni, F.; Bruni, P.; Suzuki, N.; Aihara, Y.; Croce, F. Electrospun tin-carbon nanocomposite as anode material for all solid-state lithium-ion batteries. *J. Solid State Electrochem.* **2019**, *23*, 1697–1703. [[CrossRef](#)]
30. Marinelli, L.; Cacciatore, I.; Eusepi, P.; Di Biase, G.; Morrioni, G.; Cirioni, O.; Giacometti, A.; Di Stefano, A. Viscoelastic behaviour of hyaluronic acid formulations containing carvacrol prodrugs with antibacterial properties. *Int. J. Pharm.* **2020**, *582*, 119306. [[CrossRef](#)]
31. Duan, G.; Zhang, C.; Li, A.; Yang, X.; Lu, L.; Wang, X. Preparation and Characterization of Mesoporous Zirconia Made by Using a Poly (methyl methacrylate) Template. *Nanoscale Res. Lett.* **2008**, *3*, 118–122. [[CrossRef](#)]
32. Nataraj, S.K.; Yang, K.S.; Aminabhavi, T.M. Polyacrylonitrile-based nanofibers—A state-of-the-art review. *Prog. Polym. Sci.* **2012**, *37*, 487–513. [[CrossRef](#)]
33. El-Deen, A.G.; Barakat, N.A.M.; Khalil, K.A.; Kim, H.Y. Development of multi-channel carbon nanofibers as effective electroosmotic electrodes for a capacitive deionization process. *J. Mater. Chem. A* **2013**, *1*, 11001–11010. [[CrossRef](#)]
34. Kashiwagi, T.; Hirata, T.; Brown, J.E. Thermal and Oxidative Degradation of Poly(methylMethacrylate): Molecular Weight. *Macromolecules* **1985**, *18*, 131. [[CrossRef](#)]
35. Rahaman, M.S.A.; Ismail, A.F.; Mustafa, A. A review of heat treatment on polyacrylonitrile fiber. *Polym. Degrad. Stab.* **2007**, *92*, 1421–1432. [[CrossRef](#)]
36. ICH Guideline M10 on Bioanalytical Method Validation and Study Sample Analysis. European Medicines Agency. Guideline on Bioanalytical Method Validation 30/01/2022. Available online: <https://www.ema.europa.eu/en/ich-m10-bioanalytical-method-validation-scientific-guideline> (accessed on 27 January 2023).
37. D'Angelo, V.; Tessari, F.; Bellagamba, G.; De Luca, E.; Cifelli, R.; Celia, C.; Primavera, R.; Di Francesco, M.; Paolino, D.; Di Marzio, L.; et al. Microextraction by packed sorbent and HPLC-PDA quantification of multiple anti-inflammatory drugs and fluoroquinolones in human plasma and urine. *J. Enzym. Inhib. Med. Chem.* **2016**, *31*, 110–116. [[CrossRef](#)] [[PubMed](#)]
38. Esrafil, A.; Yamini, Y.; Ghambarian, M.; Shariati, S.; Moradi, M. Measurement of fluorochinolone antibiotics from human plasma using hollow fiber liquid-phase microextraction based on carried mediated transport. *J. Liq. Chromatogr. Rel. Tech.* **2012**, *35*, 343–354. [[CrossRef](#)]
39. Zhang, J.; Chen, Z.; Tang, F.; Wu, F.; Luo, X.; Liu, G. Fabrication of highly fluorinated porphyrin-based organic frameworks decorated Fe₃O₄ nanospheres for magnetic solid phase extraction of fluoroquinolones. *Microchim. Acta* **2022**, *189*, 449. [[CrossRef](#)]
40. Qiu, Q.; Wu, Y.; Yan, X.; Li, Y.; Li, J.; Chen, Y.; Wu, D. Porous electrospun microfibers for low low-resistant solid phase extraction of fluoroquinolones in tap water, egg and milk samples. *J. Chromatogr. A* **2022**, *1661*, 462719. [[CrossRef](#)]
41. He, H.; Dong, C.; Li, B.; Dong, J.P.; Bo, T.Y.; Wang, T.L.; Feng, Y.Q. Fabrication of enrofloxacin imprinted organic-inorganic hybrid mesoporous sorbent from nanomagnetic polyhedral oligomeric silsesquioxanes for the selective extraction of fluoroquinolones in milk samples. *J. Chromatogr. A* **2014**, *1361*, 23–33. [[CrossRef](#)]
42. Wang, H.; Liu, Y.; Wei, S.; Yao, S.; Zhang, J.; Huang, H. Selective extraction and determination of fluoroquinolones in bovine milk samples with montmorillonite magnetic molecularly imprinted polymers and capillary electrophoresis. *Anal. Bioanal. Chem.* **2016**, *408*, 589–598. [[CrossRef](#)]

Disclaimer/Publisher's Note: The statements, opinions and data contained in all publications are solely those of the individual author(s) and contributor(s) and not of MDPI and/or the editor(s). MDPI and/or the editor(s) disclaim responsibility for any injury to people or property resulting from any ideas, methods, instructions or products referred to in the content.